

Holographic Schwinger effect in a rotating strongly coupled medium

Yi-ze Cai, Rui-ping Jing,* and Zi-qiang Zhang†

School of Mathematics and Physics, China University of Geosciences, Wuhan 430074, China

We perform the potential analysis for the holographic Schwinger effect in a rotating deformed AdS black-hole background. We calculate the total potential of a quark-antiquark ($Q\bar{Q}$) pair in an external electric field and evaluate the critical electric field from Dirac-Born-Infeld (DBI) action. It is shown that the inclusion of angular velocity decreases the potential barrier thus enhancing the Schwinger effect, opposite to the effect of the confining scale. Moreover, by increasing angular velocity decreases the critical electric field above which the pairs are produced freely without any suppression. Furthermore, we conclude that producing $Q\bar{Q}$ pairs would be easier in rotating medium.

I. INTRODUCTION

One of the interesting phenomenons in quantum electrodynamics (QED) is the pair production in a strong electric field, which is known as the Schwinger effect [1]. The production rate of charged particles like electron and positron was firstly computed by Schwinger for weak-coupling and weak-field [1]

$$\Gamma \sim \exp\left(\frac{-\pi m^2}{eE}\right), \quad (1)$$

where E , e and m are the external electric field, elementary electric charge and electron mass, respectively. One finds that there is no critical field in this scenario. Subsequently, Affleck et.al extended the calculation of Γ to the case for arbitrary-coupling and weak-field [2]

$$\Gamma \sim \exp\left(\frac{-\pi m^2}{eE} + \frac{e^2}{4}\right), \quad (2)$$

one finds that there is a critical field at $E_c = (4\pi/e^3)m^2 \simeq 137m^2/e$, but this critical value does not satisfy the weak-field condition, i.e., $eE \ll m^2$. Therefore, it seems that one can not get E_c under the weak-field condition. One step further, to verify the existence of E_c , one needs to work beyond the weak-field condition.

In fact, Schwinger effect is not restricted to QED, but a universal aspect of quantum field theories (QFTs) coupled to a U(1) gauge field. However, studying this effect in a QCD-like or confining theory using QFTs is difficult, because the (original) Schwinger effect is non-perturbative. Fortunately, the AdS/CFT correspondence [3–5] provides yet another way. In this approach, Semenoff and Zarembo pioneered the holographic Schwinger effect and found [6]

$$\Gamma \sim \exp\left[-\frac{\sqrt{\lambda}}{2}\left(\sqrt{\frac{E_c}{E}} - \sqrt{\frac{E}{E_c}}\right)^2\right], \quad E_c = \frac{2\pi m^2}{\sqrt{\lambda}}, \quad (3)$$

where λ is the 't Hooft coupling constant and m denotes the mass of the fundamental scalar fields in the W-boson supermultiplet, e.g., W-bosons or quarks. Interestingly, the critical value agrees with DBI result [7]. Since then, there has been a growing interest in studying holographic Schwinger effect in this direction [8–22] (for a recent review see [23]).

Here we extend the study of the (holographic) Schwinger effect in rotating medium using potential analysis. It was argued that [24–28] the quark gluon plasma (QGP) produced in (typical) noncentral heavy-ion collisions may carry a nonzero angular momentum (related to colliding nuclei) on the order of 10^4 - $10^5\hbar$ with local angular velocity in the range of 0.01-0.1 GeV. The major part of angular momentum will be taken away by the spectator nucleons, but some amount angular momentum might remain in the medium [29–31]. Certainly, there is little hope of getting a significant correction due to the angular velocity in current experiments, but it may be observed in the near future. Actually, AdS/CFT can be as insightful in this issue and various observables or quantities have already been studied. Such as drag force [32–34], jet quenching parameter [35, 36], energy loss [37–39], phase transition [40] and free energy [41].

*Electronic address: jingruiping@cug.edu.cn

†Electronic address: zhangzq@cug.edu.cn

Inspired by this, in this paper we investigate the effect of angular velocity on the Schwinger effect in a deformed AdS black-hole background. In particular, we want to know how angular velocity affects the production rate in this case. Also, this work could be regarded as an extension of [8] to the case with confining scale and angular velocity.

The paper is structured as follows. In the next section, we briefly review the rotating background considered in this work. In section 3, we perform the potential analysis for the Schwinger effect in this background and analyze how angular velocity affects the production rate. Moreover, we determine the critical field from DBI action. Finally, the results and directions for future research are discussed in section 4.

II. SETUP

Holographic QCD models like hard wall [42, 43], soft wall [44, 45] and improved holographic QCD [46–51] have achieved considerable success in describing various aspects of hadron physics. Here we adopt a type of soft wall model [45]

$$ds^2 = \frac{r^2 h(r)}{R^2} [-f(r)dt^2 + dx^2 + dy^2 + dz^2] + \frac{R^2 h(r)}{r^2 f(r)} dr^2, \quad (4)$$

with

$$f(r) = 1 - \frac{r_t^4}{r^4}, \quad h(r) = e^{c^2 R^4 / r^2}, \quad (5)$$

where R is the radius of AdS (hereafter we set $R = 1$ for convenience). r is the radial coordinate describing the 5th dimension. The horizon is $r = r_t$, defined by $f(r_t) = 0$. The boundary is $r = \infty$. Moreover, $h(r)$ refers to the warp factor, determining the characteristics of the soft wall model. c stands for the deformation parameter (or confining scale), determining the deviation from conformality.

According to [52–54], one can extend (4) to a rotating case by operating a Lorentz boost in the $t - \phi$ plane

$$t \rightarrow \gamma(t + \omega l^2 \phi), \quad \phi \rightarrow \gamma(\phi + \omega l^2 t), \quad (6)$$

with

$$\gamma = \frac{1}{\sqrt{1 - \omega^2 l^2}}, \quad (7)$$

where ϕ is the angular coordinate describing the rotation. ω represents the angular velocity. l denotes the radius of the rotating axis. Here we will focus on the qualitative results, so we simply take $l = 1 \text{ GeV}^{-1}$, similar to [40].

Given that, the corresponding transformation of (4) becomes

$$ds^2 = -m(r)dt^2 + r^2 h(r)(dx^2 + dy^2) + \frac{h(r)}{r^2 f(r)} dr^2 + n(r)(d\phi + p(r)dt)^2, \quad (8)$$

with

$$m(r) = \frac{h(r)f(r)r^2(1 - \omega^2)}{1 - f(r)\omega^2}, \quad n(r) = h(r)r^2\gamma^2(1 - f(r)\omega^2), \quad p(r) = \frac{\omega(1 - f(r))}{1 - f(r)\omega^2}. \quad (9)$$

The Hawking temperature of the black hole reads

$$T = \frac{r_t}{\pi} \sqrt{1 - \omega^2}. \quad (10)$$

Notice that for $\omega = 0$, (8) returns to (4), while for $\omega = c = 0$, it recovers to AdS black hole.

III. POTENTIAL ANALYSIS IN (HOLOGRAPHIC) SCHWINGER EFFECT

We now proceed to study the behavior of the Schwinger effect for the background (8) following [8]. As the transformation (6) is a boost in the $t - \phi$ plane, we intend to consider the $Q\bar{Q}$ pair located at $x - y$ plane e.g., the $Q\bar{Q}$ axis is supposed to be aligned in the x direction,

$$t = \tau, \quad x = \sigma, \quad y = 0, \quad \phi = 0, \quad r = r(\sigma). \quad (11)$$

The Nambu-Goto action is given by

$$S = T_F \int d\tau d\sigma \mathcal{L} = T_F \int d\tau d\sigma \sqrt{g}, \quad T_F = \frac{1}{2\pi\alpha'}, \quad (12)$$

where α' is related to λ via $\frac{R^2}{\alpha'} = \sqrt{\lambda}$. g is the determinant of the induced metric

$$g_{\alpha\beta} = g_{\mu\nu} \frac{\partial X^\mu}{\partial \sigma^\alpha} \frac{\partial X^\nu}{\partial \sigma^\beta}, \quad (13)$$

with $g_{\mu\nu}$ and X^μ the metric and target space coordinate, respectively.

Under the ansatz (11), the induced metric can be written as

$$g_{00} = -m(r) + n(r)p^2, \quad g_{01} = g_{10} = 0, \quad g_{11} = \frac{h(r)}{r^2 f(r)} \dot{r}^2 + r^2 h(r) \quad (14)$$

which yields

$$\mathcal{L} = \sqrt{A(r) + B(r)\dot{r}^2}, \quad (15)$$

with

$$A(r) = [m(r) - n(r)p^2(r)]r^2 h(r), \quad B(r) = \frac{[m(r) - n(r)p^2(r)]h(r)}{r^2 f(r)}, \quad (16)$$

where $\dot{r} = \frac{dr}{d\sigma}$.

Note that \mathcal{L} does not depend on σ explicitly, so the Hamiltonian is conserved,

$$\mathcal{L} - \frac{\partial \mathcal{L}}{\partial \dot{r}} \dot{r} = \text{Constant}. \quad (17)$$

By imposing the boundary condition

$$\frac{dr}{d\sigma} = 0, \quad r = r_c \quad (r_t < r_c < r_0), \quad (18)$$

one finds

$$\frac{dr}{d\sigma} = \sqrt{\frac{A^2(r) - A(r)A(r_c)}{A(r_c)B(r)}}, \quad (19)$$

with $A(r_c) = A(r)|_{r=r_c}$, here $r = r_0$ is an intermediate position in the bulk and this can yield a finite mass [6]. The configuration of the string world-sheet is shown in fig.1.

From (18) and (19), the inter-distance between $Q\bar{Q}$ is obtained

$$x = 2 \int_{r_c}^{r_0} dr \sqrt{\frac{A(r_c)B(r)}{A^2(r) - A(r)A(r_c)}}. \quad (20)$$

Substituting (15) and (19) into (12), the sum of Coulomb potential and static energy is obtained

$$V_{CP+E} = 2T_F \int_{r_c}^{r_0} dr \sqrt{\frac{A(r)B(r)}{A(r) - A(r_c)}}. \quad (21)$$

Next, we calculate the critical field. The DBI action is given by

$$S_{DBI} = -T_{D3} \int d^4x \sqrt{-\det(G_{\mu\nu} + \mathcal{F}_{\mu\nu})}, \quad (22)$$

with

$$T_{D3} = \frac{1}{g_s(2\pi)^3 \alpha'^2}, \quad \mathcal{F}_{\mu\nu} = 2\pi\alpha' F_{\mu\nu}, \quad (23)$$

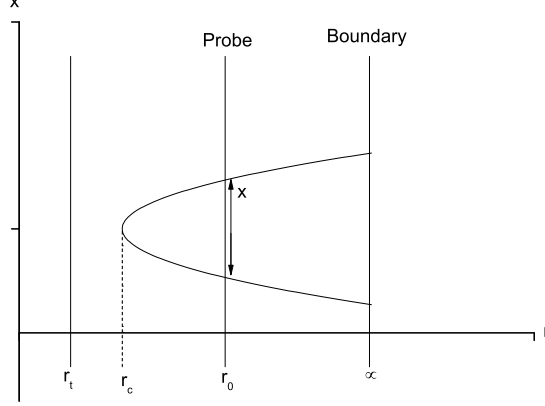


FIG. 1: String configuration.

where T_{D3} refers to the D3-brane tension.

The induced metric reads

$$G_{00} = -m(r) + n(r)p^2(r), \quad G_{11} = G_{22} = r^2h(r), \quad G_{33} = n(r), \quad G_{04} = G_{40} = n(r)p(r). \quad (24)$$

If the electric field is turned on along the x direction [8], then

$$G_{\mu\nu} + \mathcal{F}_{\mu\nu} = \begin{pmatrix} -m(r) + n(r)p^2(r) & 2\pi\alpha'E & 0 & n(r)p(r) \\ -2\pi\alpha'E & r^2h(r) & 0 & 0 \\ 0 & 0 & r^2h(r) & 0 \\ n(r)p(r) & 0 & 0 & n(r) \end{pmatrix}, \quad (25)$$

yielding

$$\det(G_{\mu\nu} + \mathcal{F}_{\mu\nu}) = r^2h(r)n(r)[(2\pi\alpha')^2E^2 - r^2h(r)m(r)]. \quad (26)$$

Plugging (26) into (22) and making the probe D3-brane located at $r = r_0$, one gets

$$S_{DBI} = -T_{D3}r_0\sqrt{h_0n_0} \int d^4x \sqrt{r_0^2h_0m_0 - (2\pi\alpha')^2E^2}, \quad (27)$$

with $h_0 = h(r)|_{r=r_0}$, $m_0 = m(r)|_{r=r_0}$, etc.

To avoid the action (27) being ill-defined, one has

$$r_0^2h_0m_0 - (2\pi\alpha')^2E^2 \geq 0, \quad (28)$$

results in

$$E \leq \frac{r_0}{2\pi\alpha'} \sqrt{h_0m_0} = T_F r_0 \sqrt{h_0m_0}. \quad (29)$$

As a result, the critical field is

$$E_c = T_F r_0 \sqrt{h_0m_0}, \quad (30)$$

one can check that E_c depends on T , c and ω .

Also, it is instructive to give the mass of the fundamental matter

$$m = T_F \int_{r_h}^{r_0} \sqrt{-\det g_{ab}} = T_F (r_0 - r_t), \quad (31)$$

on writing $m = m_0 + \Delta m$, where $m_0 = T_F r_0$ is the mass in the system without T and ω , $\Delta m = -T_F r_t$ depends on T and ω , one can rewrite E_c as

$$E_c = \frac{2\pi M^2}{\sqrt{\lambda}} \left(1 - \frac{\Delta m}{m}\right)^2 h_0 \sqrt{\frac{f_0(1-\omega^2)}{1-f_0\omega^2}}, \quad (32)$$

one can see that E_c is well defined for T and ω with fixed r_0 .

Now we are going to calculate the total potential. For convenience, we introduce some dimensionless parameters as

$$\alpha \equiv \frac{E}{E_c}, \quad y \equiv \frac{r}{r_c}, \quad a \equiv \frac{r_c}{r_0}, \quad b \equiv \frac{r_t}{r_0}. \quad (33)$$

Then the total potential becomes

$$\begin{aligned} V_{tot}(x) &= V_{CP+E} - Ex \\ &= 2ar_0T_F \int_1^{1/a} dy \sqrt{\frac{A(y)B(y)}{A(y) - A(y_c)}} \\ &\quad - 2ar_0T_F\alpha r_0 \sqrt{h_0 m_0} \int_1^{1/a} dy \sqrt{\frac{A(y_c)B(y)}{A^2(y) - A(y)A(y_c)}}, \end{aligned} \quad (34)$$

where

$$\begin{aligned} A(y) &= (m(y) - n(y)p^2(y))(ar_0y)^2 h(y), \\ B(y) &= (m(y) - n(y)p^2(y))h(y)/((ar_0y)^2 f(y)) \\ A(y_c) &= (m(y_c) - n(y_c)p^2(y_c))(ar_0)^2 h(y_c), \end{aligned} \quad (35)$$

with

$$\begin{aligned} m(y) &= \frac{h(y)f(y)(ar_0y)^2(1-\omega^2)}{1-f(y)\omega^2}, & n(y) &= h(y)(ar_0y)^2\gamma^2(1-f(y)\omega^2), & p(y) &= \frac{\omega(1-f(y))}{1-f(y)\omega^2}, \\ m(y_c) &= \frac{h(y_c)f(y_c)(ar_0)^2(1-\omega^2)}{1-f(y_c)\omega^2}, & n(y_c) &= h(y_c)(ar_0)^2\gamma^2(1-f(y_c)\omega^2), & p(y_c) &= \frac{\omega(1-f(y_c))}{1-f(y_c)\omega^2}, \\ h(y) &= e^{\frac{c^2}{(ar_0y)^2}}, & h(y_c) &= e^{\frac{c^2}{(ar_0)^2}}, & f(y) &= 1 - \left(\frac{b}{ay}\right)^4, & f(y_c) &= 1 - \left(\frac{b}{a}\right)^4, \end{aligned} \quad (36)$$

notice that by setting $c = \omega = 0$ in (34), the result of SYM [8] will be recovered.

Before proceeding, we discuss the values of some parameters. First, for comparison purposes, we take $T_F = 1$ and $b = 0.5/\sqrt{1-\omega^2}$ [8]. On the other hand, since the range of $0 \leq c/T \leq 2.5$ is most relevant for a comparison with QCD [55], we will choose the value of c in that range.

In fig.2, we plot $V_{tot}(x)$ as a function of x for various cases, where the left panel is for $c/T = 0, \omega = 0$ while the right $c/T = 2.5, \omega = 0.2 GeV$ (other cases with different values of c/T and ω have similar plots). From both panels, one can see that for $\alpha < 1$ (or $E < E_c$), the potential barrier $V_{tot}(x)$ is present, then the pair production can be described as a tunneling process. As E becomes greater, $V_{tot}(x)$ decreases gradually and vanishes at $\alpha = 1$ (or $E = E_c$). When $\alpha > 1$ ($E > E_c$), the pair production is catastrophic and the vacuum becomes catastrophically unstable. These findings are in accordance with [8].

To investigate how angular velocity affects the Schwinger effect, we plot $V_{tot}(x)$ against x with fixed c/T for different values of ω in fig.3, where the left panel is for $c/T = 0$ and the right $c/T = 2.5$. In both panels from top to bottom $\omega = 0, 0.2, 0.6 GeV$, respectively. One sees that at fixed c/T , the height and width of $V_{tot}(x)$ decrease with the increase of ω . It is known that the higher or the wider the potential barrier, the harder the produced pairs escape to infinity. Therefore, one can draw the conclusion that the inclusion of angular velocity decrease the potential barrier thus enhancing Schwinger effect. Namely, producing $Q\bar{Q}$ pairs would be easier in the presence of angular velocity. Also, by comparing the left panel with the right one, one finds that c has opposite effect, i.e., increasing c increases $V_{tot}(x)$ thus reducing Schwinger effect, consistent with the findings of [14].

Moreover, to see how angular velocity modifies the critical electric field, we plot E_c/E_{c0} versus ω in fig.4, where E_{c0} represents the critical electric field of SYM. One finds that E_c/E_{c0} decreases as ω increases, implying the inclusion of angular velocity decreases E_c thus making the tunneling process easier, in agreement with the potential analysis. Meanwhile, c has an opposite effect. In addition, one sees that E_c/E_{c0} can be smaller or larger than 1, which means the model considered in this work could provide a wider range of Schwinger effect in comparison to SYM.

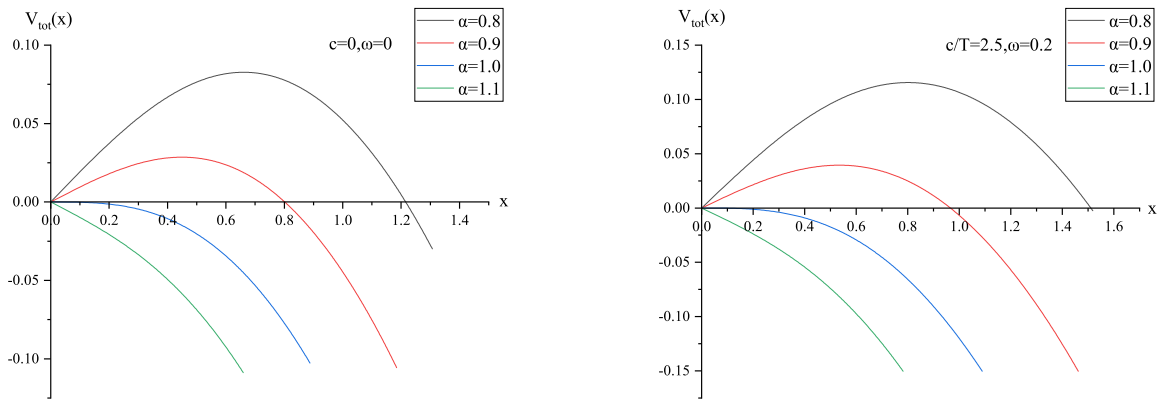


FIG. 2: $V_{tot}(x)$ versus x . Left: $c/T = 0, \omega = 0$. Right: $c/T = 2.5, \omega = 0.2 GeV$. In both panels from top to bottom $\alpha = 0.8, 0.9, 1, 1.1$, respectively.

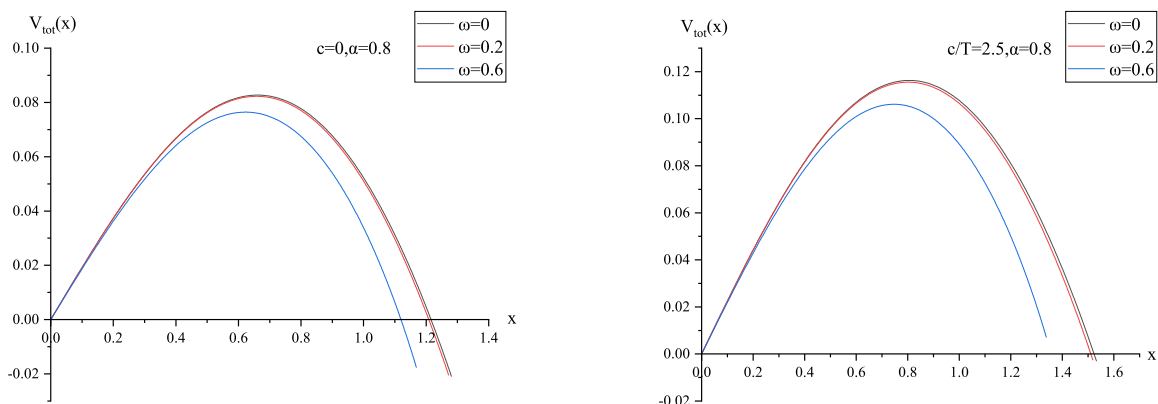


FIG. 3: $V_{tot}(x)$ versus x with $\alpha = 0.8$ and fixed c/T for different values of ω . In both plots from top to bottom $\omega = 0, 0.2, 0.6 GeV$, respectively.

IV. CONCLUSION

In this paper, we investigated the effect of angular velocity on the Schwinger effect using potential analysis in a deformed AdS black-hole background. We calculated the total potential of a $Q\bar{Q}$ pair in an external electric field and determined the critical electric field from DBI action. It is found that the inclusion of angular velocity enhances the Schwinger effect, opposite to the effect of confining scale c . Moreover, with some chosen values of ω and c/T , E_c can be smaller or larger than its counterpart of SYM, indicating the model considered here could provide theoretically a wider range of the Schwinger effect in comparison to SYM.

Interestingly, the holographic Schwinger effect has been discussed in a moving medium [13] and the results show that the presence of velocity increases the Schwinger effect as well. Taken together, one may summarize that translation and rotation have the same effect on Schwinger effect. One step further, producing $Q\bar{Q}$ pairs would be easier in moving or rotating medium. One likely explanation is that in moving or rotating backgrounds, virtual pairs may not only gain energy from the external electric field but also from the kinetic energy associated with translation and rotation. However, the exact mechanism is not very clear and needs more investigations.

Finally, it would be interesting to mention that the rotating QGP may also be described by means of 5-dimensional Kerr-AdS black hole [56]. One can study the Schwinger effect in that rotating frame as well. We hope to report our

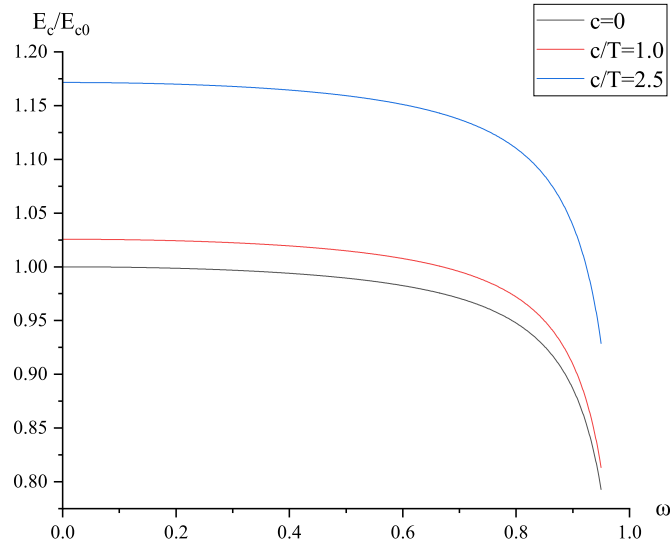


FIG. 4: Left: E_c/E_{c0} versus ω . In both plots from top to bottom $c/T = 2.5, 1, 0$, respectively.

progress in this regard in the near future.

-
- [1] J. S. Schwinger, Phys. Rev. 82 (1951) 664.
 - [2] I. K. Affleck and N. S. Manton, Nucl. Phys. B 194 (1982) 38.
 - [3] J. M. Maldacena, Adv. Theor. Math. Phys. 2, 231 (1998).
 - [4] S. S. Gubser, I. R. Klebanov and A. M. Polyakov, Phys. Lett. B 428, 105 (1998).
 - [5] O. Aharony, S. S. Gubser, J. Maldacena, H. Ooguri and Y. Oz, Phys. Rept. 323, 183 (2000).
 - [6] G. W. Semenoff and K. Zarembo, Phys. Rev. Lett. 107 (2011) 171601.
 - [7] Y. Sato and K. Yoshida, JHEP 04 (2013) 111.
 - [8] Y. Sato and K. Yoshida, JHEP 08 (2013) 002.
 - [9] Y. Sato and K. Yoshida, JHEP 09 (2013) 134.
 - [10] S. Chakraborty and B. Sathiapalan, Nucl. Phys. B 890 (2014) 241.
 - [11] M. Ghodrati, Phys. Rev. D 92, 065015 (2015).
 - [12] K. B. Fadafan and F. Saiedi, Eur. Phys. J. C (2015) 75:612.
 - [13] Z.-q. Zhang, D. f. Hou and G. Chen, Eur.Phys.J.A 53 (2017) 3, 51.
 - [14] Y. Ding, Z.-q. Zhang, Chin.Phys.C 45 (2021) 1, 013111.
 - [15] Z.-q. Zhang, X. R. Zhu and D. f. Hou, Phys. Rev. D 101, 026017 (2020).
 - [16] L. Shahkarami, M. Dehghani, P. Dehghani, Phys. Rev. D 97, 046013 (2018).
 - [17] Z. R. Zhu, D. f. Hou, Xun Chen, Eur. Phys. J. C (2020) 80:550.
 - [18] W. Fischler, P. H. Nguyen, J. F. Pedraza, W. Tangarife, Phys. Rev. D 91, 086015 (2015).
 - [19] K. Hashimoto and T. Oka, JHEP 10 (2013) 116.
 - [20] K. Hashimoto, T. Oka, and A. Sonoda, JHEP 06 (2014) 085.
 - [21] X. Wu, JHEP 09 (2015) 044.
 - [22] K. Ghoroku, M. Ishihara, JHEP 09 (2016) 011.
 - [23] D. Kawai, Y. Sato, K. Yoshida, Internat. J. Modern Phys. A 30 (2015) 1530026.
 - [24] The STAR Collaboration, Nature 548 (2017) 62-65.
 - [25] Z. T. Liang and X. N. Wang, Phys. Rev. Lett. 94, 102301 (2005); 96, 039901(E) (2006).
 - [26] F. Becattini, F. Piccinini, J. Rizzo, Phys. Rev. C 77, 024906 (2008).
 - [27] X. G. Huang, P. Huovinen, and X. N. Wang, Phys. Rev. C 84, 054910 (2011).
 - [28] L. G. Pang, H. Petersen, Q. Wang, and X. N. Wang, Phys. Rev. Lett. 117, 192301 (2016).
 - [29] M. I. Baznat, K.K. Gudima, A.S. Sorin, O.V. Teryaev, Phys. Rev. C 93, 031902 (2016).
 - [30] D. E. Kharzeev, J. Liao, S. A. Voloshin and G. Wang, Prog. Part. Nucl. Phys. 88, 1 (2016).
 - [31] Y. Jiang, Z. W. Lin, and J. Liao, Phys. Rev. C 94, 044910 (2016); 95, 049904(E) (2017).

- [32] I. Ya. Arefeva, A. Bagrov and A. Koshelev, JHEP 07 (2013)170.
- [33] I. Ya. Arefeva, A. A. Golubtsova and E. Gourgoulhon, JHEP 04 (2021) 169.
- [34] A. N. Atmaja and K. Schalm, JHEP 1104 (2011) 070.
- [35] J. Sadeghi and B. Pourhassan, Int. J. Theor. Phys. 50, 2305 (2011).
- [36] B. McInnes, arXiv:1710.07442 [hep-ph].
- [37] K. B. Fadafan, H. Liu, K. Rajagopal, Eur. Phys. J. C 61 (2009) 553.
- [38] M. Atashi, K. B. Fadafan, Phys. Lett. B 800 (2020) 135090
- [39] D. f. Hou, M. Atashi, K. B. Fadafan, Z.q. Zhang, Phys. Lett. B 817 (2021) 136279
- [40] X. Chen, L. Zhang, D. Li, D. Hou and M. Huang, JHEP 07 (2021) 132.
- [41] J. Zhou, X. Chen, Y-Q Zhao, and J.l. Ping, Phys. Rev. D 102, 126029 (2020).
- [42] J. Erlich, E. Katz, D. T. Son and M. A. Stephanov, Phys. Rev. Lett. 95, 261602 (2005).
- [43] J. Polchinski, M. J. Strassler, JHEP 05 (2003) 012.
- [44] A. Karch, E. Katz, D. T. Son and M. A. Stephanov, Phys. Rev. D 74, 015005 (2006).
- [45] P. Colangelo, F. Giannuzzi, and S. Nicotri, Phys. Rev. D 83, 035015 (2011).
- [46] J. P. Shock, F. Wu, Y-L. Wu and Z-F. Xie, JHEP 03 (2007) 064.
- [47] A. Stoffers and I. Zahed, Phys. Rev. D 83, (2011) 055016.
- [48] D. n. Li and M. Huang, JHEP 11 (2013) 088.
- [49] D. n. Li, S. He, M. Huang and Q. S. Yan, JHEP 09 (2011) 041.
- [50] S. He, M. Huang and Q. S. Yan, JHEP, Phys. Rev. D 83, 045034 (2011).
- [51] S. He, S. Y. Wu, Y. Yang and P. H. Yuan, JHEP 04 (2013) 093.
- [52] M. B. Gaete, L. Guajardo, and M. Hassaine, JHEP 04 (2017) 092.
- [53] C. Erices and C. Martinez, Phys. Rev. D 97, 024034 (2018).
- [54] A. M. Awad, Classical Quantum Gravity 20, 2827 (2003).
- [55] H. Liu, K. Rajagopal, and Y. Shi, JHEP 0808 (2008) 048.
- [56] S.W.Hawking, C.J.Hunter and M.Taylor-Robinson, Phys.Rev. D 59 (1999) 064005.